

PEARL: Performance-Enhanced Aggregated Representation Learning

Wenhui Li^{1*}, Shijing Gong^{2*}, and Xinyu Zhang^{1,2†}

Academy of Mathematics and Systems Science, Chinese Academy of Sciences¹;
School of Management, University of Science and Technology of China²

September 30, 2025

Abstract

Representation learning is a key technique in modern machine learning that enables models to identify meaningful patterns in complex data. However, different methods tend to extract distinct aspects of the data, and relying on a single approach may overlook important insights relevant to downstream tasks. This paper proposes a performance-enhanced aggregated representation learning method, which combines multiple representation learning approaches to improve the performance of downstream tasks. The framework is designed to be general and flexible, accommodating a wide range of loss functions commonly used in machine learning models. To ensure computational efficiency, we use surrogate loss functions to facilitate practical weight estimation. Theoretically, we prove that our method asymptotically achieves optimal performance in downstream tasks, meaning that the risk of our predictor is asymptotically equivalent to the theoretical minimum. Additionally, we derive that our method asymptotically assigns nonzero weights to correctly specified models. We evaluate our method on diverse tasks by comparing it with advanced machine learning models. The experimental results demonstrate that our method consistently outperforms baseline methods, showing its effectiveness and broad applicability in real-world machine learning scenarios.

Running title: PEARL

Key words: Representation learning | Model averaging | Machine learning

*Wenhui Li and Shijing Gong contributed equally to this work.

†Corresponding author: xinyu@amss.ac.cn

1 Introduction

Modern data analysis frequently involves high-dimensional, large-scale, structured, unstructured, and multi-modal datasets. Representation learning plays a crucial role in extracting information-rich features from such data, and it has become a fundamental technique across various machine learning domains, including natural language processing (Vaswani et al., 2017), computer vision (Krizhevsky et al., 2017), and speech recognition (Radford et al., 2023), and has also shown success in bioinformatics (Garruss et al., 2021) and neuroscience (Wybo et al., 2023). Traditional representation learning methods, including factor analysis and multi-dimensional scaling, have been extended to deep learning-based approaches (Xie et al., 2020). Deep learning-based approaches employ multi-layer nonlinear transformations to progressively capture abstract and hierarchical features from raw data. For instance, early neural network models demonstrated success in visual pattern recognition (LeCun et al., 1998; Krizhevsky et al., 2017). More recent transformer-based architectures (Vaswani et al., 2017) form the basis of modern large language models capable of learning representations and processing natural language text (Brown et al., 2020; Ouyang et al., 2022).

The performance of machine learning methods heavily relies on the choice of data representations (Bengio et al., 2013). With the large pool of available representation learning methods, some studies have treated representation choice as a model selection problem, aiming to pick the most effective pretrained representation for a given task (Nguyen et al., 2020; You et al., 2021). However, relying on a single representation learning method may ignore complementary information that other methods may capture. Moreover, the effectiveness of a selected representation learning model can vary substantially across data and task conditions (Ericsson et al., 2021; Agostinelli et al., 2022). To address these issues, it is essential to develop strategies that aggregate multiple representation learning methods.

In this paper, we propose a model averaging framework called performance-enhanced aggregated representation learning (PEARL), designed to improve downstream performance by combining diverse representations. Model averaging is a popular technique that addresses the uncertainty of choosing models (Hjort and Claeskens, 2003; Hansen, 2007), and recently works have proven success in complex models including random forest (Chen et al., 2024) and neural networks (Zeng and den Broeck, 2023; Wang et al., 2025). However, existing efforts are often confined to specific model structures or task domains. This raises the need for a more general model averaging framework that can accommodate both simple models and deep complex architectures, while being applicable across diverse tasks. Representation learning provides a natural bridge toward this goal since representation learning is a core component of most machine learning methods.

PEARL consists of two stages. In the first stage, a set of foundation representation learning (FRL) models, which are either trained from scratch or adapted from pretrained encoders such as BERT (Devlin et al., 2019) and GPT (Brown et al., 2020), transform raw inputs into representation vectors. These representations, individually or combined through integration strategies, form a pool of candidate representation sets. In the second stage, each candidate set is linked to the target task through a downstream predictor (e.g., a linear model

or neural network). The final output of PEARL is obtained by averaging these predictions, with weights estimated by a cross-validation-based weighting criterion.

The term ‘‘performance-enhanced’’ in PEARL reflects its effectiveness in both computational feasibility and theoretical guarantees. For the computational simplicity, a key design principle of PEARL is the weighting procedure. To accommodate diverse downstream tasks, the weighting criterion is formulated on the basis of a generalized loss function. However, directly optimizing certain loss functions may introduce non-smooth or non-convex optimization challenges. To enable efficient and stable weight computation, PEARL employs surrogate loss functions as approximations to original loss functions. Moreover, PEARL adopts a linear weighting scheme rather than nonlinear deep aggregation, thereby further reducing computational cost and preserving interpretability.

We establish two main theoretical guarantees for PEARL. First, from the perspective of downstream task performance, we prove the asymptotic optimality of the PEARL predictor. Specifically, the predictive risk of PEARL converges to the lowest possible risk defined by the original loss. This result ensures that PEARL performs at least as well as any single FRL in the pool and other linear combinations of FRLs, such as simple ensemble. Second, from the perspective of weight interpretability, we prove weight consistency. Specifically, when the candidate pool contains correctly specified models, PEARL asymptotically assigns all weight to them. This property demonstrates that PEARL is able to identify and prioritize well-specified models among candidates. Together, these results provide a solid theoretical foundation for both the effectiveness and the interpretability of PEARL across diverse downstream tasks.

The rest of the paper is organized as follows. Section 2 presents the model framework including representation learning process, downstream task analysis, and weight choice criterion. Section 3 shows the asymptotic optimality and weight consistency of the proposed method PEARL. Section 4 shows one numerical simulation study and four real-world datasets. Section 5 summarizes our work and discusses the future works. In supplementary materials, Appendix A gives the proofs of theoretical results, and Appendix B shows the implementation details of experiments.

2 Method

Suppose that there is a set of different artificial intelligence techniques that map between the predictors $x \in \mathcal{X}$ and the outputs $y \in \mathcal{Y}$. We aim to predict an output in a downstream task given a new predictor. The predictor space \mathcal{X} is generalized to accommodate a broad spectrum of scenarios. It may include structured elements (e.g., numerical vectors) and unstructured elements (e.g., text, images).

2.1 Representation Learning Process

A representation learning function f maps each predictor $x \in \mathcal{X}$ to a p -dimensional representation vector $z \in \mathcal{R}^p$, i.e., $f : \mathcal{X} \rightarrow \mathcal{R}^p, x \mapsto z$. Representation learning methods vary based

on the type of input data and the analyst’s preferences. For structured data, techniques such as principal component analysis (PCA) are commonly used for dimensionality reduction. For image data, methods like convolutional autoencoders (AE) or contrastive learning approaches (e.g., SimCLR (Chen et al., 2020)) have proven effective in extracting meaningful representations. For text data, models such as Word2Vec or transformer-based approaches (e.g., BERT) are frequently employed to generate semantic embeddings. Moreover, each method involves specific hyperparameters (e.g., the number of principal components in PCA, network architecture details in autoencoder or transformer models) that can lead to variations in the learned representations, thereby constituting different representation learning techniques.

We consider M representation learning models as our FRL models, each mapping the input space \mathcal{X} to a model-specific p_m -dimensional vector space \mathcal{R}^{p_m} , i.e., for the m -th model,

$$f_m : \mathcal{X} \rightarrow \mathcal{R}^{p_m}, \quad x \mapsto z_{(m)}.$$

The function space is defined by \mathcal{F} . These models are trained on the unlabeled dataset $\mathcal{D}^u = \{x'_i \in \mathcal{X}\}_{i=1}^N$, where x'_i is the i -th unlabeled sample and N denotes the number of unlabeled samples. Suppose the m -th FRL model employs a representation learning loss $U_m(\cdot)$ on \mathcal{D}^u to obtain

$$\hat{f}_m = \arg \min_{f \in \mathcal{F}} \sum_{i=1}^N U_m(f(x'_i)).$$

For example, let us illustrate the PCA process to extract representations for panel data. Define the data matrix by $X' = (x'_1, \dots, x'_N)^T \in \mathcal{R}^{N \times T}$. PCA seeks a linear map that gets the p_m -dimensional latent factors: $z'_{i,(m)} = f_m(x'_i) = B_m^T x'_i$, where $B_m \in \mathcal{R}^{T \times p_m}$ is the parameter matrix. Let $Z'_{(m)} = (z'_{1,(m)}, \dots, z'_{n,(m)})^T$. Then $\hat{f}_m(x) = \hat{B}_{(m)}^T x$ for any vector $x \in \mathcal{X}$, where $\hat{B}_{(m)}$ is calculated by solving a constrained least squares loss function after centering the columns of X' :

$$\begin{aligned} (\hat{Z}'_{(m)}, \hat{B}_m) &= \arg \min_{B, Z} (\|X - ZB^T\|_F^2), \\ \text{s.t. } T^{-1} \sum_{i=1}^N z_i z_i^T &= I_{p_m} \text{ and } B^T B \text{ diagonal,} \end{aligned}$$

where z_i is the i -th row of Z and $\hat{Z}'_{(m)}$ is the estimator of $Z'_{(m)}$. The loss $U_m(\cdot)$ can be a U -embedding loss function designed for unannotated data (Dai et al., 2022) and can be tailored for different scenarios including contrastive loss or generative modeling objectives (Chen et al., 2020; He et al., 2020; Kingma and Welling, 2013). In each case, the structure of f_m and the dimension p_m in the resulting representations might differ.

2.2 Downstream Task Analysis

In this subsection, we focus on the downstream task analysis on a labeled dataset $D^l = \{(x_i, y_i) \in \mathcal{X} \times \mathcal{Y}\}_{i=1}^n$, where n is the number of labeled samples. Specifically, this subsection consists of two parts: constructing a set of candidate representations and developing a model averaging predictor to estimate the output for a new input $x_{\text{new}} \in \mathcal{X}$.

With M learned FRL models $\{\hat{f}_1, \hat{f}_2, \dots, \hat{f}_M\}$, each \hat{f}_m maps $x_i \in \mathcal{X}$ to a vector in \mathcal{R}^{p_m} .

Symbolically,

$$\widehat{z}_{i,(m)} = \widehat{f}_m(x_i) \text{ for } i = 1, \dots, n, \quad m = 1, \dots, M,$$

where $\widehat{z}_{i,(m)} \in \mathcal{R}^{p_m}$ is defined as the foundation representation vector under the m -th FRL model. By collecting these vectors for all n samples, we form the foundation representation matrix $\widehat{Z}_{(m)} = (\widehat{z}_{1,(m)}, \dots, \widehat{z}_{n,(m)})^T \in \mathcal{R}^{n \times p_m}$ for the m -th FRL model.

Next, we introduce candidate representation sets that include both the foundation representations directly learned by FRL models and additional representations obtained through fusion or combinatorial techniques. To avoid notational confusion, with a total of J candidate representation sets ($J \geq M$), for $1 \leq i \leq n$, we denote the j -th candidate representation vector by $\widehat{z}_{i,[j]}$ and their corresponding matrices $\widehat{Z}_{[j]} = (\widehat{z}_{1,[j]}, \dots, \widehat{z}_{n,[j]})^T$ for $1 \leq j \leq J$. Note that the subscript bracket for notations of candidate representation sets is $[\]$ and is different from $(\)$ for the foundation representation set $\widehat{z}_{i,(m)}$ for $1 \leq m \leq M$. Let p_j be the dimension of the vector $\widehat{z}_{i,[j]}$ and therefore $\widehat{Z}_{[j]} \in \mathcal{R}^{n \times p_j}$.

For additional representation sets, one simple way is to consider a simple fusion technique that concatenates the foundation representations: $(\widehat{z}_{i,(1)}^T, \widehat{z}_{i,(2)}^T, \dots, \widehat{z}_{i,(M)}^T)^T \in \mathcal{R}^p$, where $p = \sum_{m=1}^M p_m$. The corresponding fusion matrix is $(\widehat{Z}_{(1)}, \widehat{Z}_{(2)}, \dots, \widehat{Z}_{(M)})$. This approach is common in deep learning to integrate complementary information from various models (Zhang et al., 2020). In addition to simple fusion, we provide Example 1 below to illustrate several methods for constructing additional representation sets.

- Example 1.**
1. *Foundation Set Combinations.* For instance, when $M = 3$ and each $p_m = 2$, using all non-empty subsets of the three foundation representation sets yields $J = 2^M - 1 = 7$ candidate representation sets. This includes individual foundation sets, pairwise concatenations, and the complete concatenation of all three. Mathematically, the candidate representation sets are $\widehat{Z}_{[j]} = \widehat{Z}_{(j)}$ for $j = 1, 2, 3$; $\widehat{Z}_{[4]} = (\widehat{Z}_{(1)}, \widehat{Z}_{(2)})$; $\widehat{Z}_{[5]} = (\widehat{Z}_{(1)}, \widehat{Z}_{(3)})$; $\widehat{Z}_{[6]} = (\widehat{Z}_{(2)}, \widehat{Z}_{(3)})$; and $\widehat{Z}_{[7]} = (\widehat{Z}_{(1)}, \widehat{Z}_{(2)}, \widehat{Z}_{(3)})$.
 2. *Fusion Matrix Columns Combinations.* For instance, when $M = 3$ and each $p_m = 2$, concatenating all foundation representations forms a fusion matrix with $p = 6$ columns. Taking every non-empty subset of these columns gives $J = 2^p - 1 = 63$ candidate representation sets. Each combinatorial subset of the six columns in the fusion matrix forms a candidate representation set. Although this method yields a larger set of candidates, it also poses challenges in terms of computational complexity and potential redundancy.
 3. *Domain knowledge-based selection.* This method emphasizes the integration of expert insights to select or weight candidate representations. For example, in asset pricing, well-established asset factors may be combined with factors learned via deep learning to enhance interpretability and performance (Feng et al., 2024). This approach helps mitigate the combinatorial explosion in candidate sets by narrowing the focus to the most relevant representations.

After we construct the J candidate representation sets, we build the relationship between

candidate representations and the output on the labeled dataset \mathcal{D}^l . For the j -th candidate representation set, a function g_j that maps \mathcal{R}^{p_j} onto \mathcal{Y} is:

$$g_j : \widehat{z}_{i,[j]} \mapsto y_i \text{ and } g_j \in \mathcal{G},$$

where \mathcal{G} is the class of considered functions. The model g_j could be a linear regression, a logistic regression, or a more complex nonlinear model depending on the problem types. The function g_j is learned using $(\widehat{z}_{i,[j]}, y_i)_{i=1}^n$ and the corresponding estimated function is defined by \widehat{g}_j for $1 \leq j \leq J$. When the dimensionality of the representations is too large, g_j can be a sparsity-inducing function to reduce the dimensionality. For example, the regularization method employed in Li and Li (2022) can be utilized.

Consider a new observation $x_{\text{new}} \in \mathcal{X}$ and our goal is to predict its label y_{new} . We first generate M foundation representation sets by applying M FRL models on x_{new} , and then construct J candidate representation sets for x_{new} , denoted as $\{\widehat{z}_{\text{new},[j]}\}_{j=1}^J$. For each $1 \leq j \leq J$, the candidate model generates an output as follows:

$$\widehat{y}_{\text{new},[j]} = \widehat{g}_j(\widehat{z}_{\text{new},[j]}).$$

We propose a model averaging approach to aggregate these J outputs by assigning weights to each of them. Specifically, the model averaging predictor is defined as:

$$\widehat{y}_{\text{new}}(\mathbf{w}) = \sum_{j=1}^J w_j \widehat{y}_{\text{new},[j]}, \quad (1)$$

where w_j is the weight assigned to the j -th output, and the weight vector $\mathbf{w} = (w_1, \dots, w_J)^T$ lies in the simplex \mathbf{w} satisfies that $\mathbf{w} \in \mathcal{W} = \{\mathbf{w} \in [0, 1]^J : \sum_{j=1}^J w_j = 1\}$. The weight assignment for diverse candidate models is critical in model averaging, as it reflects the relative predictive power of each candidate model. Next, we discuss how to tune the weights for different downstream tasks.

2.3 Weight Choice Criterion

For downstream tasks, the criteria for model evaluation and their corresponding loss functions often differ. Our paper aims to build a generalized framework that can adaptively handle different kinds of loss functions based on various machine-learning-based candidate models. A simple but naive approach is to construct the weight criterion that is directly based on the targeted loss function. The weights are tuned on the labeled dataset by

$$\widehat{\mathbf{w}} = \operatorname{argmin}_{\mathbf{w} \in \mathcal{W}} n^{-1} \sum_{i=1}^n L(y_i, \widehat{y}_i(\mathbf{w})), \quad (2)$$

where $\widehat{y}_i(\mathbf{w}) = \sum_{j=1}^J w_j \widehat{y}_{i,[j]}$ and $L(\cdot, \cdot)$ is a loss function that measures the difference between the true responses and the weighted predictions. However, the weighting criterion (2) has two problems. First, many loss functions, particularly in complex or classification problems, can be non-convex or non-differentiable (e.g., the 0-1 loss or certain robust loss functions). These properties hinder the direct application of gradient-based optimization methods, potentially

leading to suboptimal solutions or convergence issues. Second, optimizing the loss over the all training samples may cause the model to fit the noise or idiosyncratic patterns in the training data rather than capturing the underlying general patterns. This may increase the risk of overfitting problem (John Lu, 2010).

For the computational complexity problem in (2), surrogate loss functions that are convex and differentiable are often employed. For some surrogate losses, their connection to the original loss is supported by theoretical guarantees, such as classification calibration, consistency in risk minimization, or upper bounds on the excess risk measured by the original loss (Mao et al., 2023). For example, in classification task, the hinge loss (Cortes, 1995), the logistic loss (Zhu and Hastie, 2005), and the ψ -loss (Shen et al., 2003) are often employed as smooth approximations for the zero-one classification loss. These surrogate losses not only facilitate optimization but also have been shown to preserve desirable theoretical properties under certain conditions, such as minimizing the surrogate loss leads to minimization of the original loss under suitable conditions. In addition, if the original loss function is computational friendly, such as the mean squared error in regression tasks, it is entirely reasonable to use the original loss function without substitution.

For the overfitting problem in (2), we propose a cross-validation-based weight tuning algorithm (Algorithm 1). Let $S = \{1, \dots, n\}$ denote the index set, which is divided into K equally sized folds: $S = \bigcup_{k=1}^K S_k$, where S_k is the index set in the k -th fold. For the j -th candidate model and each $k \in \{1, \dots, K\}$, we refit the model g_j using the dataset $\{(\hat{z}_{i,[j]}, y_i)\}_{i \in S \setminus S_k}$. The resulting refitted function of g_j excluding the k -fold is denoted by $\tilde{g}_j^{(-k)}$. Then $\tilde{g}_j^{(-k)}$ is applied on $\{\hat{z}_{i,[j]}\}_{i \in S_k}$ to obtain $\tilde{y}_{i,[j]} = \tilde{g}_j^{(-k)}(z_{i,[j]})$ with $i \in S_k$. By aggregating the predictions from all folds, we get the cross-validation-based prediction for all labeled samples under the j -th candidate model, denoted by $\tilde{y}_{[j]} = (\tilde{y}_{1,[j]}, \dots, \tilde{y}_{n,[j]})^T$. Finally, we estimate the weights by

$$\hat{\mathbf{w}} = \operatorname{argmin}_{\mathbf{w} \in \mathcal{W}} n^{-1} \sum_{i=1}^n V(y_i, \tilde{y}_i(\mathbf{w})), \quad (3)$$

where V is the surrogate loss function for the original loss function L , $\hat{\mathbf{w}} = (\hat{w}_1, \dots, \hat{w}_J)^T$, and $\tilde{y}_i(\mathbf{w}) = \sum_{j=1}^J w_j \tilde{y}_{i,[j]}$.

By (3), we plug in the obtained $\hat{\mathbf{w}}$ in (1) to derive our PEARL prediction for the label of the new observation x_{new} :

$$\hat{y}_{\text{new}}(\hat{\mathbf{w}}) = \sum_{j=1}^J \hat{w}_j \hat{y}_{\text{new},[j]}. \quad (4)$$

2.4 PEARL for Multimodal Data

This part illustrates how the proposed method PEARL is applied to multimodal representation learning. In many practical applications, data are available in multiple modalities—such as images and text for news articles or sequences of images, audio, and text for YouTube videos. The proposed method PEARL can effectively combine representations learned from each modality.

Algorithm 1 K -Fold cross-validation weight criterion

- 1: **Input:** Labeled data $D^l = \{(x_i, y_i)\}_{i=1}^n$; Number of folds K ; M FRL models $\{\hat{f}_1, \dots, \hat{f}_M\}$; Surrogate loss function V .
- 2: Construction of the representations: For $m \in \{1, \dots, M\}$ and $i \in \{1, \dots, n\}$, $\hat{z}_{i,(m)} = \hat{f}_m(x_i)$; for $j \in \{1, \dots, J\}$ generate $\hat{z}_{i,[j]}$.
- 3: Cross-validation weight tuning: Partition index set $S = \{1, \dots, n\}$ into K folds: $S = \bigcup_{k=1}^K S_k$.
- 4: **for** $j \leftarrow 1$ **to** J **do**;
- 5: **for** $k \leftarrow 1$ **to** K **do**
- 6: $D_{\text{train}} \leftarrow \{(\hat{z}_{i,[j]}, y_i)\}_{i \in S \setminus S_k}$;
- 7: Train the prediction model $\tilde{g}_j^{(-k)}$ on D_{train} ;
- 8: Obtain $\tilde{y}_{i,[j]} = \tilde{g}_j^{(-k)}(\hat{z}_{i,[j]})$ for $i \in S_k$.
- 9: Summarize all folds: $\tilde{y}_{[j]} = (\tilde{y}_{1,[j]}, \dots, \tilde{y}_{n,[j]})^T$.
- 10: The weighted prediction is given by $\tilde{y}_i(\mathbf{w}) = \sum_{j=1}^J w_j \tilde{y}_{i,[j]}$. where $\mathbf{w} = (w_1, \dots, w_J)^T \in \mathcal{W}$
- 11: Solve for the weights by minimizing

$$\hat{\mathbf{w}} = \operatorname{argmin}_{\mathbf{w} \in \mathcal{W}} \frac{1}{n} \sum_{i=1}^n V(y_i, \tilde{y}_i(\mathbf{w})).$$

- 12: **Output:** $\hat{\mathbf{w}}$.
-

Suppose our predictor consists of S distinct modalities, abstractly represented as

$$\mathcal{X} = \mathcal{X}^1 \cup \mathcal{X}^2 \cup \dots \cup \mathcal{X}^S,$$

where the union symbol is used in an abstract sense. In practice, integrating these heterogeneous data sources may require a Cartesian product or another specific form of fusion, depending on how the features interact. We consider a large collection of N unlabeled samples, $\mathcal{D}^u = \{x'_i \in \mathcal{X} : i = 1, \dots, N\}$, to train a total of M foundational representation learning (FRL) models. These FRL models are designed to learn representations from the multimodal input data, and they can operate on single modalities or combinations thereof. For illustration, consider two example FRL models for the input $x = (x^1, \dots, x^S) \in \mathcal{X}$:

$$\begin{aligned} f_1 &: \mathcal{X}^1 \rightarrow \mathcal{R}^{p_1}, & x^1 &\mapsto z_{(1)}, \\ f_2 &: (\mathcal{X}^2, \mathcal{X}^3) \rightarrow \mathcal{R}^{p_2}, & (x^2, x^3) &\mapsto z_{(2)}. \end{aligned}$$

Here, f_1 represents FRL models that focus on individual modalities, while f_2 represents those built to capture joint information from a combination of modalities (see, e.g., (Ngiam et al., 2011; Shekhar et al., 2014; Gu et al., 2017)). The complete set of trained FRL models is denoted as $\{\hat{f}_1, \dots, \hat{f}_M\}$.

For the downstream task, we assume that there are n labeled samples forming the dataset $D^l = \{(x_i, y_i) \in \mathcal{X} \times \mathcal{Y} : i = 1, \dots, n\}$ where each $x_i = (x_i^1, x_i^2, \dots, x_i^S)$ is a multimodal input and y_i is the corresponding label. For example, the foundational representations for sample

x_i obtained via the first two FRL models are $\widehat{z}_{i,(1)} = \widehat{f}_1(x_i^1)$ and $\widehat{z}_{i,(2)} = \widehat{f}_2(x_i^2, x_i^3)$, respectively. After extracting representations from all M FRL models, we generate J candidate representation sets, denoted by $\widehat{z}_{i,[j]}$ for $i = 1, \dots, n$ and $j = 1, \dots, J$. The subsequent steps of our methodology follow the procedure outlined in our main algorithm, where we derive cross-validation weights, fit the prediction models, and make prediction for any new observation $x_{\text{new}} \in \mathcal{X}$.

3 Theoretical Results

In this section, we demonstrate the theoretical efficiency of our proposed method, PEARL, by analyzing two key aspects. First, we show that the risk of the PEARL predictor in downstream tasks is asymptotically equivalent to the theoretical minimum risk. Second, we establish that the sum of the weights assigned to the correctly specified models converges to one.

For the representation learning process, let f_m^* represent the optimal representation learning function that maps from \mathcal{X} to \mathcal{R}^{p_m} under the given representation learning loss $U_m(\cdot)$, that is $f_m^* = \arg \min_{f \in \mathcal{F}} \mathbb{E}[U_m(f(x))]$ with $x \in \mathcal{X}$ for $1 \leq m \leq M$. For $x \in \mathcal{X}$, we then define the optimal foundation representation for x under the m -th FRL model as $z_{(m)}^* = f_m^*(x)$ for $1 \leq m \leq M$. By concatenating the optimal representations from all M FRL models, we obtain the fused optimal representations $z^* = (z_{(1)}^{*T}, z_{(2)}^{*T}, \dots, z_{(M)}^{*T})^T$ by directly augmenting the optimal representations from FRL models. By following procedure in Example 1, we denote the optimal candidate representations by $z_{[j]}^*$ for $1 \leq j \leq J$ by applying the candidate construction procedure to optimal foundation representations.

For the downstream task analysis process, for $1 \leq j \leq J$, let $g_j^* = \arg \min_{g \in \mathcal{G}} \mathbb{E}[L(y_i, g(z_{[j]}^*))]$ be the optimal learning function using the j -th candidate representation set. Let a function $h^*(x, \mathbf{w}) = \sum_{j=1}^J w_j g_j^*(z_{[j]}^*)$ be the model averaging value of outputs derived from optimal candidate representations and optimal downstream task learning function, as $z_{[j]}^*$ depends on x . Define $\mathbf{w}^* = (w_1, \dots, w_J)^T$ that satisfies $\mathbf{w}^* = \arg \min_{\mathbf{w} \in \mathcal{W}} E[L(y, h^*(x, \mathbf{w}))]$. Analogously, for the estimated values, define $\widehat{h}(x, \mathbf{w}) = \sum_{j=1}^J w_j \widehat{g}_j(\widehat{z}_{[j]})$.

Assumption 1. *Suppose there exist constants $\mu > 0$ and $c_1 > 0$ such that when $\mathbb{E}[V(y, \widehat{h}(x, \mathbf{w}))] - \mathbb{E}[V(y, h^*(x, \mathbf{w}^*))] \leq \epsilon$ for $\mathbf{w} \in \mathcal{W}$ and a small error $\epsilon > 0$, then*

$$\mathbb{E}[L(y, \widehat{h}(x, \mathbf{w}))] - \mathbb{E}[L(y, h^*(x, \mathbf{w}^*))] \leq c_1 \epsilon^\mu.$$

Assumption 1 requires that a small bias bound in the surrogate function V can translate into a relatively small bias bound in the true loss function L . The polynomial relationship between the bias bound of V and L is also adapted in Assumption A1 in Dai et al. (2022). Such conditions hold in many standard machine-learning problems where V is carefully designed to approximate L , such that by controlling the bias of the surrogate loss, we also control the bias of the true loss.

Assumption 2. For each $1 \leq i \leq n$ and $\mathbf{w} \in \mathcal{W}$, if $\mathbb{E}[V(y_i, \tilde{y}_i(\mathbf{w})) - V(y_i, y_i^*(\mathbf{w}))] \leq \epsilon$ for some small error $\epsilon > 0$, then there exist constants $\kappa > 0$ and $c_2 > 0$ such that,

$$\text{var}[V(y_i, \tilde{y}_i(\mathbf{w})) - V(y_i, y_i^*(\mathbf{w}))] \leq c_2 \epsilon^\kappa.$$

Assumption 2 bounds the variance of loss difference between $\tilde{y}_i(\mathbf{w})$ and $y_i^*(\mathbf{w})$ if the expected difference is small in the surrogate function V . This assumption requires a mild smoothness for V , where the constant κ reflects the smoothness. Assumption 2 is similar to Assumption A2 in Dai et al. (2022).

Assumption 3. For any $\mathbf{w} \in \mathcal{W}$, $\text{var}(V(y, h^*(x, \mathbf{w}))) \leq c_3$, where c_3 is a positive constant.

Assumption 3 requires that variances of the surrogate loss of model averaging estimator derived from optimal representations and downstream task learning function is bounded by a positive constant. It indicates that the data distribution and the model do not produce arbitrarily large fluctuations in the surrogate loss.

Assumption 4. For two predicted outputs y' and y'' , it has $|V(y, y') - V(y, y'')| \leq K(y) \|y' - y''\|$, where $K(y)$ is independent of y' and y'' , and satisfies $\mathbb{E}^{1/2}(|K(y)|^2) \leq c_4$ for some positive constant c_4 .

Assumption 4 requires the smoothness of the surrogate function. It is similar to Assumption 2 in (Yu et al., 2024), which poses the stochastic equicontinuity on the measure of divergence in the original loss function, and Assumption A in (Zhu et al., 2016) and Assumption 4.2 in (Bi et al., 2018), the two of which pose the smoothness on the likelihood function derived the original loss function. Compared with these smoothness assumptions imposed on L , Here, we apply it to V , thereby broadening the class of possible original losses that lack such smoothness but still allow a suitably chosen V to meet this requirement. This assumption is often key for establishing uniform convergence of empirical loss processes, as it ensures small differences in the predicted output lead to small changes in the surrogate loss measure.

Assumption 4 can be satisfied when the surrogate loss is a *margin-based* loss. For hinge loss $V(y, f) = \max\{0, 1 - yy'\}$ under a binary classification setting with $y \in \{-1, +1\}$, it satisfies that

$$|\max\{0, 1 - yy'\} - \max\{0, 1 - yy''\}| \leq |(1 - yy') - (1 - yy'')| = |y||y' - y''| \leq |y' - y''|,$$

where $K(y) = 1$. For the logistic loss (cross-entropy loss) $V(y, y') = \log(1 + e^{-yy'})$ with $y \in \{-1, +1\}$, its derivative with respect to y' satisfies

$$\frac{\partial}{\partial y'} \log(1 + e^{-yy'}) = -\frac{ye^{-yy'}}{1 + e^{-yy'}},$$

whose absolute value is bounded by 1. Hence, the logistic loss is Lipschitz in y' with a constant at most $|y|$ and $K(y) = 1$ in Assumption 4. More generally, many margin-based losses take the form $V(y, y') = \phi(yy')$ for some convex and often smooth function ϕ , including

the exponential loss, the smoothed hinge loss, and various robust surrogates. In each case, one typically finds a bounded derivative with respect to y' , thus admitting a finite Lipschitz constant $K(y)$ that depends at most on $|y|$. For binary classification with $y \in \{-1, +1\}$, we immediately get $|y| = 1$, yielding a constant $K(y) \leq 1$. In multi-class or other extended settings, one can assume $\|y\| \leq C_y$ with high probability, ensuring $\mathbb{E}[K(y)^2] < c_4$.

Assumption 5. *There exists a sequence $\alpha_{N,n}$ depending on N and n , such that*

$$\max_{1 \leq j \leq J} \mathbb{E}^{1/2}(\|\widehat{g}_j(\widehat{z}_{[j]}) - g_j^*(z_{[j]}^*)\|^2) = O(\alpha_{N,n})$$

and

$$\max_{1 \leq j \leq J} \mathbb{E}^{1/2}(\|\widetilde{g}_j(\widehat{z}_{[j]}) - g_j^*(z_{[j]}^*)\|^2) = O(\alpha_{N,n}).$$

Assumption 5 shows the maximum error bound of J candidate estimators and their corresponding CV estimators to the limiting values for J candidate models. In practice, $\alpha_{N,n}$ may shrink to 0 as $N, n \rightarrow \infty$, reflecting the convergence rate of estimators and their corresponding CV estimators. The requirement holds *uniformly* over $j = 1, \dots, J$, which is natural in model-averaging contexts where multiple candidate models are considered.

The error bound of $\widehat{g}_j(\widehat{z}_{i,[j]})$ can be decomposed by the approximation error (the discrepancy introduced by training downstream learning function) and the estimation error (the discrepancy introduced by estimating representations) as follows

$$\|\widehat{g}_j(\widehat{z}_{i,[j]}) - g_j^*(z_{i,[j]}^*)\| \leq \underbrace{\|\widehat{g}_j(z_{i,[j]}^*) - g_j^*(z_{i,[j]}^*)\|}_{\text{approximation error}} + \underbrace{\|\widehat{g}_j(\widehat{z}_{i,[j]}) - \widehat{g}_j(z_{i,[j]}^*)\|}_{\text{estimation error}}. \quad (5)$$

The approximation error depicts the ability of model \widehat{g}_j in Step 2 to approximate the optimal model g_j^* . The approximation error can potentially be reduced by using more flexible model specifications, which allow experts to better tailor the model to the data. However, increasing model flexibility also introduces the risk of overfitting. Overfitting occurs when the model becomes too closely aligned with the specific patterns in the training data, which may lead to poor performance when applied to new and unseen data. The estimation error arises due to the representation learning process in Step 1. If the used function \widehat{g} falls in the Lipschitz-continuous function space, then the estimation error is bounded by $c^L \|\widehat{z}_{i,[j]} - z_{i,[j]}^*\|$ with a positive Lipschitz constant c^L . Analogously, the estimation error of $\widetilde{g}_j(\widehat{z}_{i,[j]})$ can be decomposed similar to (5) and it is assumed that the cross validated estimator inherits the convergence rate of the original estimator.

In addition, the framework can be extended to encompass commonly used pretrained models as foundation models. Unlike the assumption in the original formulation, where all foundation models are trained on the same unlabeled dataset, these pretrained models may be trained on different unsupervised datasets. Subsequently, they use the learned representations for downstream task analysis. Specifically, let \mathcal{D}_m^u denote the unsupervised dataset for the m -th foundation model, with a sample size of N_m . To generalize the framework for

these pretrained models, we modify Assumption 5 by setting $N = \max_{1 \leq m \leq M} N_m$.

3.1 Asymptotic Optimality

Define the risk function of model averaging predictor with respect to the label of a new observation x_{new} by

$$R_L(\mathbf{w}) = \mathbb{E}\{L(y_{\text{new}}, \widehat{y}_{\text{new}}(\mathbf{w}))\} = \mathbb{E}\{L(y_{\text{new}}, \sum_{j=1}^J w_j \widehat{g}_j(\widehat{z}_{\text{new}, [j]}))\}. \quad (6)$$

Now, let's define the risk function of the weighted predictor using the limiting values of each model's prediction:

$$R_L^*(\mathbf{w}) = \mathbb{E}\{L(y_{\text{new}}, y_{\text{new}}^*(\mathbf{w}))\} = \mathbb{E}\{L(y_{\text{new}}, \sum_{j=1}^J \omega_j g_j^*(z_{\text{new}, [j]}^*))\}. \quad (7)$$

We define the surrogate risk function $R_V(\mathbf{w})$ of our model averaging estimator by replacing $L(\cdot)$ with $V(\cdot)$ in (6). The corresponding risk function with limiting values $R_V^*(\mathbf{w})$ is then defined by replacing $L(\cdot)$ with $V(\cdot)$ in (7). Define the infimum risk of $R_L^*(\mathbf{w})$ by $\xi_L = \inf_{\mathbf{w} \in \mathcal{W}} R_L^*(\mathbf{w})$, and the infimum risk of $R_V^*(\mathbf{w})$ by $\xi_V = \inf_{\mathbf{w} \in \mathcal{W}} R_V^*(\mathbf{w})$.

Assumption 6. $\xi_V^{-1} \xi_L = O(1)$ and $\xi_V^{-1} \max\{\alpha_{N,n}^{\kappa/2} n^{-1/2}, \alpha_{N,n}^{\kappa}, \alpha_{N,n}^{\mu}\} = o(1)$.

Assumption 6 contains two parts. Part I = $\xi_V^{-1} \xi_L = O(1)$ keeps minimal possible surrogate risk on the same order with the minimal possible true loss. It is a mild or non-degenerate condition ensuring that improvements on the surrogate side can be translated to improvements on the true loss. To put it in another words, if ξ_V is extremely larger than ξ_L , it may imply that even the best surrogate solution performs poor in the true loss, making it pointless to minimize V instead of L . Part II = $\xi_V^{-1} \max\{\alpha_{N,n}^{\kappa/2} n^{-1/2}, \alpha_{N,n}^{\kappa}, \alpha_{N,n}^{\mu}\} = o(1)$ means that the minimal possible surrogate risk ξ_V diverges at the rate faster than $\max\{\alpha_{N,n}^{\kappa/2} n^{-1/2}, \alpha_{N,n}^{\kappa}, \alpha_{N,n}^{\mu}\}$. The term $\alpha_{N,n}$ measures the approximation error and estimation error of the two stages, and the term $\alpha_{N,n}^{\kappa/2} n^{-1/2}$ arises by controlling the cross-validation and sample-average difference under polynomial variance bounds, and $\alpha_{N,n}^{\mu}$ arises by converting the risk difference of surrogate loss to that of the true loss.

Theorem 1. *Under Assumptions 1-6, we have*

$$\frac{R_L(\widehat{\mathbf{w}})}{\inf_{\mathbf{w} \in \mathcal{W}} R_L(\mathbf{w})} \xrightarrow{p} 1.$$

Theorem 1 shows the asymptotic optimality of PEARL predictor of y_{new} in terms of risk. It means that PEARL predictor can asymptotically outperform or at least match any convex combination of candidate models when $\mathbf{w} \in \mathcal{W}$. A commonly used convex combination is the simple model averaging with equal weights, $\mathbf{w} = (M^{-1}, \dots, M^{-1})^T$. Additionally, the PEARL predictor can also outperform or match any single candidate model, as the weight

vector with one element equal to one and others zero lies in \mathcal{W} . The details of the theoretical assumptions and proof can be found in the Appendix.

3.2 Weight Consistency

Next, we prove the consistency of the weights that the estimated weights are assigned to the correctly specified models when such models are included in the averaging pool. The concept of the correctly specified candidate models refers that $g_j^*(z_{\text{new},[j]}^*) = \mathbb{E}(y_{\text{new}}|x_{\text{new}})$ for the j -th candidate model.

Let $\mathcal{D} \subset \{1, \dots, J\}$ be a subset of $\{1, \dots, J\}$ that contains all the index of the correctly specified candidate models. Define $\hat{\tau} = \sum_{j \in \mathcal{D}} \hat{w}_j$ be the sum of weights assigned to the correctly specified candidate models. Assume that that \mathcal{D} is not empty, and it means that at least one correctly specified model is included in the candidate model set, and therefore we only need to prove that $\hat{\tau} \rightarrow 1$ to show the consistency of weights. In addition, since if all candidate models are correctly specified, then the result $\hat{\tau} = 1$ is directly derived, we assume that $\mathcal{D} \neq \{1, \dots, J\}$. Define $\mathcal{W}_s = \{\mathbf{w} \in \mathcal{W} : \sum_{j \notin \mathcal{D}} w_j = 1\}$ be a weight set that assigns all weights on the misspecified models .

Assumption 7. For every $\mathbf{w} \in \mathcal{W}$, there are $R_V^*(\mathbf{w}) \geq c_5 \|y_{\text{new}}^*(\mathbf{w}) - \mathbb{E}(y_{\text{new}}|x_{\text{new}})\|^2$, for some positive constant c_5 .

Assumption 7 is similar to Assumption 5 in (Yu et al., 2024) which assumes the lower bound on the risk of true loss, and we focus on the surrogate one. Next, let us show how commonly used surrogate losses—squared error, logistic (cross-entropy), and hinge loss imply Assumption 7. For squared-error loss where $V(y_{\text{new}}, y_{\text{new}}^*(\mathbf{w})) = L(y_{\text{new}}, y_{\text{new}}^*(\mathbf{w})) = (y_{\text{new}}^*(\mathbf{w}) - y_{\text{new}})^2$, By the usual orthogonality argument for squared error,

$$R_V^*(\mathbf{w}) = \mathbb{E}[(y_{\text{new}}^*(\mathbf{w}) - y_{\text{new}})^2] = \mathbb{E}[(y_{\text{new}}^*(\mathbf{w}) - \mathbb{E}[y_{\text{new}} | x_{\text{new}}])^2] + \mathbb{E}[(\mathbb{E}[y_{\text{new}} | x_{\text{new}}] - y_{\text{new}}^*(\mathbf{w}))^2].$$

Therefore, we have $R_V^*(\mathbf{w}) \geq \|y_{\text{new}}^*(\mathbf{w}) - \mathbb{E}[y_{\text{new}} | x_{\text{new}}]\|^2$.

For logistic (cross-entropy) loss with $y_{\text{new}} \in \{-1, 1\}$, we know $V(y_{\text{new}}, y_{\text{new}}^*(\mathbf{w})) = \log(1 + \exp(-y_{\text{new}} y_{\text{new}}^*(\mathbf{w})))$ and $R_V^*(\mathbf{w}) = \mathbb{E}[\log(1 + \exp\{-y_{\text{new}} y_{\text{new}}^*(\mathbf{w})\})]$. Since $\ell(m) = \log(1 + e^m)$ is strictly convex relative to m . Then

$$\begin{aligned} & \log(1 + \exp(-y_{\text{new}} y_{\text{new}}^*(\mathbf{w}))) - \log(1 + \exp(-y_{\text{new}} \mathbb{E}(y_{\text{new}}|x_{\text{new}}))) \\ & \geq c(y_{\text{new}} \mathbb{E}(y_{\text{new}}|x_{\text{new}}) - y_{\text{new}} y_{\text{new}}^*(\mathbf{w}))^2 \\ & \geq c(\mathbb{E}(y_{\text{new}}|x_{\text{new}}) - y_{\text{new}}^*(\mathbf{w}))^2 \end{aligned}$$

for some constant $c > 0$. Then we have

$$R_V^*(\mathbf{w}) - \mathbb{E}[\log(1 + e^{-y_{\text{new}} \mathbb{E}(y_{\text{new}}|x_{\text{new}})})] \geq c \mathbb{E}[|y_{\text{new}}^*(\mathbf{w}) - \mathbb{E}(y_{\text{new}}|x_{\text{new}})|^2]$$

Since the term $[\log(1 + e^{-y_{\text{new}} \mathbb{E}(y_{\text{new}}|x_{\text{new}})})]$ is always larger than 0, then the logistic loss satisfies Assumption 7.

For hinge loss with $y_{\text{new}} \in \{-1, +1\}$, we have $V(y_{\text{new}}, y_{\text{new}}^*(\mathbf{w})) = \max\{0, 1 - y_{\text{new}} y_{\text{new}}^*(\mathbf{w})\}$. By piecewise linearity and local strong-convexity that

$$R_V^*(\mathbf{w}) - \mathbb{E}[V(y_{\text{new}}, \mathbb{E}(y_{\text{new}}|x_{\text{new}}))] \geq c\mathbb{E}[\|y_{\text{new}}^*(\mathbf{w}) - \mathbb{E}(y_{\text{new}}|x_{\text{new}})\|^2],$$

where the term $\mathbb{E}[V(y_{\text{new}}, \mathbb{E}(y_{\text{new}}|x_{\text{new}}))]$ is a constant that does not depend on \mathbf{w} . Therefore, the hinge loss still satisfies Assumption 7.

Assumption 8. $\max\{\alpha_{N,n}^{\kappa/2} n^{-1/2}, \alpha_{N,n}^{\kappa}\} \{\inf_{\mathbf{w} \in \mathcal{W}_s} \|\sum_{j \notin \mathcal{D}} w_j [y_{i,[j]}^* - \mathbb{E}(y_{\text{new}}|x_{\text{new}})]\|^2\}^{-1} = o(1)$.

Assumption 8 means that the divergence speed of minimum risk of averaging across all misspecified models is faster than $\max\{\alpha_{N,n}^{\kappa/2} n^{-1/2}, \alpha_{N,n}^{\kappa}\}$.

Theorem 2. *If Assumptions 1-5 and 7-8 are satisfied, then we have $\hat{\tau} \rightarrow 1$.*

Theorem 2 shows that the nonzero weights will asymptotically be put on the correctly specified candidate models when at least one correctly specified model exists in the candidate set. This result implies that, PEARL will asymptotically concentrate on the models whose optimal predicted values coincide with the conditional expectation.

4 Experiments

This section presents a simulation study and four real-world datasets to demonstrate the effectiveness of PEARL across different tasks and domains. The simulation study tests a non-linear regression data generating process for the regression task. Four real-world datasets consist of MNIST (Deng, 2012) and CIFAR-10 (Krizhevsky, 2009) for image classification, Polarity (Pang and Lee, 2004) for sentiment analysis, and Wine Review* for multi-modal learning. A summary of experiments and their corresponding FRL methods is presented in Table 1, with detailed implementation information provided in Appendix B. For classification tasks in our experiments, we use the cross entropy (CE) loss as the surrogate function V , and other tasks use the squared loss function when calculating the weights.

We compare PEARL with following baseline methods: Best, Fusion, SA-FRL, SA-cand, and MS. Each of these methods provides a different strategy for aggregating or selecting models. Best reports the best individual FRL model with the best performance, serving as a benchmark to assess whether leveraging multiple FRL models improves performance. Fusion refers to the direct fusion method that uses the combination of representations of all considered FRL models. Fusion shows the result of using all representations without weighting any individual models. SA-FRL is a simple averaging method that equally averages predictions of all individual FRL models. SA-cand is another simple averaging method that equally averages the predictions of all candidate models. The difference between SA-FRL and SA-cand lies in the set of models being averaged. MS is a model selection method that selects the best candidate model based on cross-validation. MS is compared with PEARL to show the advantages of using a weighted average of models rather than selecting a single model.

*<https://www.kaggle.com/datasets/zynicide/wine-reviews>

Table 1: Summary of FRL methods applied to different tasks and datasets.

Task Type & Dataset	FRL Methods
Synthetic dataset: A synthetic regression task with a nonlinear data generating process.	PCA KPCA (Gaussian Kernel) KPCA (Polynomial Kernel) KPCA (Sigmoid Kernel) KPCA (Cosine Kernel)
MNIST: An image classification task that classifies handwritten digits into one of ten categories.	AE (CNN encoder) VAE (CNN encoder) SimCLR (MLP encoder) SimCLR (CNN encoder) Original Image
CIFAR-10: An image classification task that classifies color images into one of ten categories.	AE (ResNet encoder) VAE (ResNet encoder) SimCLR (CNN encoder) SimCLR (ResNet encoder)
Polarity: A text classification task that predicts sentiment polarity (positive or negative) from movie reviews.	CountVectorizer TF-IDF Vectorizer Word2Vec Doc2Vec GloVe BERT
Wine Review: A multi-modal regression task that predicts the quality of wines.	PCA (Numerical Modality) VAE (Numerical Modality) BERT (Textual Modality) GPT-2 (Textual Modality)

4.1 Synthetic Dataset

This section presents a simulation study on a regression task to evaluate our proposed methods. The data generating process is defined as:

$$y_i = \beta_0 + \beta_1 x_{i1} + \beta_2 x_{i2} + \alpha_1 x_{i1}^2 + \alpha_2 x_{i2}^2 + \gamma x_{i1} x_{i2} + \sin^2(x_{i1}) + \epsilon_i, \quad (8)$$

where observed predictors $\mathbf{x}_i = (x_{i1}, x_{i2})^T$ are independent identically distributed (i.i.d.) from $\mathcal{N}(\mathbf{0}, \mathbf{I})$, and $\epsilon_i \sim \mathcal{N}(0, \sigma^2)$. The coefficients $(\beta_0, \beta_1, \beta_2, \alpha_1, \alpha_2, \gamma)$ are drawn independently from $\mathcal{N}(0, 0.09)$. We vary noise levels with $\sigma \in \{0.1, 0.5, 0.9, 1.5\}$ and labeled sample sizes $n \in \{100, 200, 400, 800\}$ for labeled data, fixing unlabeled sample size $N = 2000$. Each configuration is repeated 100 times.

We adopt kernel principal component analysis (KPCA) (Mika et al., 1998) with five kernels shown in Table 1 as FRL models to extract representations from predictors. These yield five foundation representation sets, from which we construct $J = 2^5 - 1 = 31$ candidate sets by all non-empty combinations (see Example 1). For each candidate set, a linear regression is fit on the labeled dataset to predict the target variable.

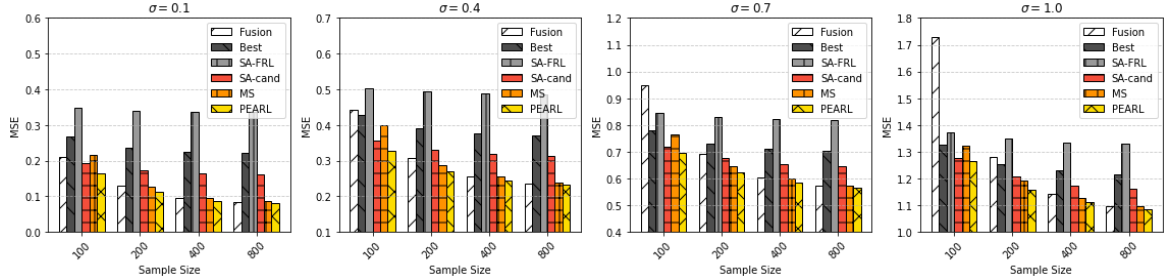


Figure 1: Synthetic-data results

The results in Fig. 1 reveal that our method outperforms the baseline methods in most cases. As the noise level increases, which is proportional to σ , the performance of the Fusion and MS methods deteriorates more rapidly than that of PEARL, particularly when $n = 100$ or 200. For larger sample sizes ($n = 500$ or 1000), PEARL substantially outperforms Best, SA-FRL and SA-cand. These results demonstrate that PEARL mitigates overfitting in small sample sizes and maximizes predictive performance in larger datasets.

4.2 MNIST Dataset

We also evaluate PEARL on the MNIST benchmark for image classification. We use similar configuration for FRL methods, except that the ResNet encoders are replaced with CNN ones. For downstream classification, we employ either a simple MLP or multinomial logistic regression. As shown in Table 2, PEARL consistently outperforms baselines in MNIST dataset. The implementation details are provided in Appendix B.

We evaluate PEARL on the MNIST benchmark for image classification, consisting of 70k grayscale digit images (60k training, 10k testing, 28×28 pixels). We use two types of FRL methods, AE and SimCLR (Chen et al., 2020), each with MLP and CNN encoders, and also include the raw images as an additional representation set. Therefore, we have $M = 5$ FRL and $J = 31$ candidate representation sets via Example 1. For downstream classification, we employ either a simple MLP or multinomial logistic regression. Experiments are conducted with $n \in \{500, 1000, 3000, 6000\}$ labeled samples, repeated 50 times with random subsets, while FRL models are pretrained once on the full training set to enable reuse across tasks.

For evaluation, we use the standard 10000-image test set and measure the performance of different methods using three metrics: classification accuracy (Acc), CE, and mean squared error (MSE) between the true and predicted labels. In Table 2 and all subsequent experiments, the best results are highlighted in bold red, while the second-best are underlined blue.

Table 2 demonstrates that PEARL consistently outperforms baseline methods across all metrics and sample sizes, indicating superior classification performance and enhanced calibration. The implementation details are provided in Appendix B.

Table 2: Results of different methods on MNIST dataset

	n	Fusion	Best	SA-FRL	SA-cand	MS	PEARL
Acc	300	94.647 (0.509)	95.390 (0.385)	94.140 (0.501)	94.863 (0.467)	<u>96.242 (0.478)</u>	96.355 (0.451)
	600	95.949 (0.309)	96.016 (0.236)	95.064 (0.295)	96.062 (0.282)	<u>96.984 (0.286)</u>	97.086 (0.237)
	1500	97.066 (0.204)	96.879 (0.165)	96.095 (0.191)	97.241 (0.193)	<u>97.625 (0.187)</u>	97.762 (0.159)
	3000	97.570 (0.143)	97.316 (0.145)	96.578 (0.133)	97.844 (0.120)	<u>97.939 (0.165)</u>	98.090 (0.122)
CE	300	0.170 (0.016)	0.152 (0.015)	0.238 (0.011)	0.178 (0.011)	<u>0.122 (0.015)</u>	0.121 (0.013)
	600	0.132 (0.011)	0.127 (0.007)	0.196 (0.006)	0.140 (0.006)	<u>0.096 (0.009)</u>	0.094 (0.006)
	1500	0.099 (0.008)	0.099 (0.005)	0.161 (0.003)	0.106 (0.004)	<u>0.074 (0.006)</u>	0.071 (0.004)
	3000	0.082 (0.006)	0.085 (0.003)	0.146 (0.002)	0.090 (0.002)	<u>0.064 (0.005)</u>	0.059 (0.003)
MSE	300	0.008 (0.001)	0.007 (0.001)	0.011 (0.001)	0.008 (0.001)	<u>0.006 (0.001)</u>	0.006 (0.001)
	600	0.006 (0.000)	0.006 (0.000)	0.009 (0.000)	0.006 (0.000)	<u>0.005 (0.000)</u>	0.004 (0.000)
	1500	0.004 (0.000)	0.005 (0.000)	0.007 (0.000)	0.005 (0.000)	<u>0.004 (0.000)</u>	0.003 (0.000)
	3000	0.004 (0.000)	0.004 (0.000)	0.007 (0.000)	0.004 (0.000)	<u>0.003 (0.000)</u>	0.003 (0.000)

4.3 CIFAR-10 Dataset

The CIFAR-10 dataset contains 60,000 color images of size 32×32 pixels, divided into 10 object categories (airplane, automobile, bird, cat, deer, dog, frog, horse, ship, and truck). The dataset is split into 50,000 training images and 10,000 test images, with 6,000 images per class. We use $M = 4$ FRL models as shown in Table 1, which create $J = 15$ candidate representation sets via Example 1. For AE, VAE, and SimCLR we use ResNet encoders, where SimCLR is also instantiated with a CNN encoder. See Appendix D for implementation details. For downstream classification, we employ either a simple MLP or multinomial logistic regression. Experiments are conducted with $n \in \{300, 500, 1500, 3000\}$ labeled samples, repeated 100 times with random subsets, while FRL models are pretrained once on the full training set to enable reuse across tasks. For evaluation, we use three metrics: classification accuracy (Acc), CE, and mean squared error (MSE) between the true and predicted labels/probabilities.

As shown in Table 3, PEARL consistently outperforms baselines across all metrics and sample sizes, demonstrating superior classification accuracy and better calibration. Compared with MS, which successfully selects the single FRL model with the highest performance since MS has the same performance with Best, PEARL further improves the results. This demonstrates the clear advantage of combining different models rather than relying on a single one. Moreover, when compared with SA-FRL and SA-cand, PEARL also achieves superior performance. This highlights that different models contribute unequally to the downstream task, and assigning task-specific weights is more effective than applying equal weights. Finally, relative to Fusion, the weighted averaging strategy in PEARL yields better results. This confirms that learning to weight different representation groups is more beneficial than simply concatenating them.

4.4 Polarity Dataset

We use the Polarity v2.0 dataset (Pang and Lee, 2004), a standard benchmark for sentiment analysis containing 2000 movie reviews evenly split between positive and negative labels.

Table 3: Results of different methods on CIFAR-10 dataset

	n	Fusion	Best	SA-FRL	SA-cand	MS	PEARL
Acc (%)	300	42.129 (1.938)	<u>53.379 (0.836)</u>	42.125 (2.441)	43.839 (1.992)	<u>53.379 (0.836)</u>	53.825 (0.831)
	600	48.748 (1.600)	<u>56.133 (0.529)</u>	48.449 (1.416)	50.791 (1.527)	<u>56.133 (0.529)</u>	57.028 (0.521)
	1500	56.389 (0.706)	<u>58.432 (0.380)</u>	53.726 (0.775)	57.663 (0.701)	<u>58.432 (0.380)</u>	60.186 (0.375)
	3000	60.342 (0.456)	59.518 (0.251)	55.791 (0.493)	<u>60.704 (0.456)</u>	59.817 (0.566)	61.928 (0.356)
CE	300	2.589 (0.303)	<u>1.292 (0.023)</u>	1.587 (0.031)	1.614 (0.075)	<u>1.292 (0.023)</u>	1.282 (0.023)
	600	1.983 (0.220)	<u>1.212 (0.011)</u>	1.475 (0.013)	1.399 (0.041)	<u>1.212 (0.011)</u>	1.190 (0.012)
	1500	1.350 (0.047)	<u>1.149 (0.006)</u>	1.404 (0.006)	1.233 (0.013)	<u>1.149 (0.006)</u>	1.104 (0.007)
	3000	1.140 (0.015)	<u>1.120 (0.004)</u>	1.378 (0.005)	1.173 (0.007)	<u>1.114 (0.010)</u>	1.054 (0.006)
MSE	300	0.087 (0.005)	<u>0.060 (0.001)</u>	0.071 (0.002)	0.072 (0.003)	<u>0.060 (0.001)</u>	0.059 (0.001)
	600	0.075 (0.004)	<u>0.057 (0.000)</u>	0.067 (0.001)	0.064 (0.002)	<u>0.057 (0.000)</u>	0.056 (0.000)
	1500	0.060 (0.001)	<u>0.054 (0.000)</u>	0.064 (0.000)	0.057 (0.001)	<u>0.054 (0.000)</u>	0.052 (0.000)
	3000	0.053 (0.001)	<u>0.053 (0.000)</u>	0.063 (0.000)	0.054 (0.000)	<u>0.053 (0.001)</u>	0.050 (0.000)

The task is binary sentiment classification. We consider $M = 6$ FRL models, including CountVectorizer, TF-IDF (term frequency-inverse document frequency), Doc2Vec (Le and Mikolov, 2014), Word2Vec (Mikolov et al., 2013), BERT, and GloVe (Pennington et al., 2014). Among these, BERT and GloVe are pre-trained models, while the others are trained from scratch. For downstream classification, we apply either a simple MLP or logistic regression on the learned representations, using a 70%-30% train-test split repeated 10 times for robustness.

Table 4: Comparison of different methods on polarity dataset

	Fusion	Best	SA	PEARL-CE
Acc (%)	83.587 (1.445)	<u>87.745 (1.113)</u>	86.233 (1.392)	88.873 (1.173)
CE	0.482 (0.045)	<u>0.308 (0.014)</u>	0.423 (0.009)	0.291 (0.013)
MSE	0.126 (0.010)	<u>0.092 (0.005)</u>	0.128 (0.004)	0.086 (0.005)

Given the high dimensionality of CountVectorizer and TF-IDF, no additional candidate sets are constructed, yielding $M = J = 6$. In this case, SA-cand reduces to SA-FRL, and MS is dominated by Best, so both are omitted from comparison. As shown in Table 4, PEARL consistently outperforms the remaining baselines, demonstrating its effectiveness even without additional candidate sets.

4.5 Wine Review Dataset

We evaluate PEARL in a multi-modal setting using the Wine Review dataset (approximately 130k records), where each review contains unstructured text and structured attributes (variety, location, winery, and price). The task is to predict the wine quality score as a continuous outcome. For representation learning, we use PCA and VAEs (Kingma and Welling, 2013) for numerical attributes, and pre-trained BERT and GPT-2 (Radford et al., 2019) for text, trained on 10k unlabeled samples. Linear regression is applied to labeled sets of size $n \in \{100, 200, 500, 1000, 2000\}$, with evaluation on 5k test samples. Each split is repeated 10

times, and performance is assessed by average MSE.

Table 5: Comparison of different methods on wine review dataset

n	Best	Fusion	SA-repr	SA-cand	MS	PEARL
100	7.296 (0.588)	<u>6.159 (0.537)</u>	26.849 (56.176)	17.670 (28.147)	6.468 (0.592)	5.726 (0.384)
200	7.596 (0.451)	5.678 (0.353)	5.251 (0.291)	4.973 (0.274)	6.203 (0.792)	<u>5.103 (0.334)</u>
500	7.124 (0.335)	6.497 (0.350)	5.441 (0.264)	<u>5.371 (0.268)</u>	6.557 (0.393)	4.920 (0.193)
1000	6.730 (0.264)	10.336 (0.659)	<u>5.407 (0.206)</u>	6.171 (0.286)	6.878 (0.550)	5.332 (0.247)
2000	5.496 (0.136)	14.210 (1.002)	<u>4.147 (0.131)</u>	4.416 (0.127)	5.043 (0.299)	3.659 (0.084)

From Table 5, across most sample sizes, PEARL achieves the lowest MSE compared with both single-modality baselines (Best) and other averaging strategies, showing clear advantages in integrating heterogeneous representations from multi-modal datasets. These results underscore that PEARL not only improves prediction accuracy but also maintains robustness in the challenging multi-modal setting, highlighting its strong generalizability beyond unimodal tasks.

5 Summary

In this work, we introduce a theoretically grounded aggregation method for representation learning based on frequentist model averaging. The proposed framework is widely applicable and highly general, accommodating tasks ranging from matrix/tensor decomposition to nonlinear representation learning in deep neural networks. This broad scope underscores its ability to bridge interpretable statistical tools with modern AI techniques, making it suitable for diverse real-world applications.

Future work can focus on developing online learning algorithms that enable the model ensemble to adapt in real-time to evolving data streams, ensuring it remains responsive and robust in non-stationary environments. Additionally, it is appealing to applying the framework to deep learning in decision-making applications in areas such as autonomous driving, medical diagnostics, or financial risk assessment.

References

- Agostinelli, A., M. Pándy, J. Uijlings, T. Mensink, and V. Ferrari (2022). How stable are transferability metrics evaluations? In *European Conference on Computer Vision*, pp. 303–321. Springer.
- Bengio, Y., A. Courville, and P. Vincent (2013). Representation learning: A review and new perspectives. *IEEE Transactions on Pattern Analysis and Machine Intelligence* 35(8), 1798–1828.
- Bi, X., A. Qu, and X. Shen (2018). Multilayer tensor factorization with applications to recommender systems. *The Annals of Statistics* 46(6B), 3308–3333.

- Brown, T., B. Mann, N. Ryder, M. Subbiah, J. D. Kaplan, P. Dhariwal, A. Neelakantan, P. Shyam, G. Sastry, A. Askell, et al. (2020). Language models are few-shot learners. *Advances in Neural Information Processing Systems* 33, 1877–1901.
- Chen, T., S. Kornblith, M. Norouzi, and G. Hinton (2020). “A simple framework for contrastive learning of visual representations”. In H. D. III and A. Singh (Eds.), *Proceedings of the 37th International Conference on Machine Learning*, pp. 1597–1607. PMLR.
- Chen, X., D. Yu, and X. Zhang (2024). Optimal weighted random forests. *Journal of Machine Learning Research* 25(320), 1–81.
- Cortes, C. (1995). Support-vector networks. *Machine Learning* 20, 273–297.
- Dai, B., X. Shen, and J. Wang (2022). Embedding learning. *Journal of the American Statistical Association* 117(537), 307–319.
- Deng, L. (2012). The mnist database of handwritten digit images for machine learning research. *IEEE Signal Processing Magazine* 29(6), 141–142.
- Devlin, J., M.-W. Chang, K. Lee, and K. Toutanova (2019). “BERT: Pre-training of deep bidirectional transformers for language understanding”. In *Proceedings of the 2019 Conference of the North American Chapter of the Association for Computational Linguistics: Human Language Technologies*, pp. 4171–4186.
- Ericsson, L., H. Gouk, and T. M. Hospedales (2021). How well do self-supervised models transfer? In *Proceedings of the IEEE/CVF Conference on Computer Vision and Pattern Recognition*, pp. 5414–5423.
- Feng, G., J. He, N. G. Polson, and J. Xu (2024). Deep learning in characteristics-sorted factor models. *Journal of Financial and Quantitative Analysis* 59(7), 3001–3036.
- Garruss, A. S., K. M. Collins, and G. M. Church (2021). Deep representation learning improves prediction of laci-mediated transcriptional repression. *Proceedings of the National Academy of Sciences* 118(27), e2022838118.
- Gu, Z., B. Lang, T. Yue, and L. Huang (2017). Learning joint multimodal representation based on multi-fusion deep neural networks. In *Neural Information Processing: 24th International Conference, ICONIP 2017, Guangzhou, China, November 14-18, 2017, Proceedings, Part II 24*, pp. 276–285. Springer.
- Hansen, B. E. (2007). Least squares model averaging. *Econometrica* 75(4), 1175–1189.
- He, K., H. Fan, Y. Wu, S. Xie, and R. Girshick (2020). “Momentum contrast for unsupervised visual representation learning”. In *Proceedings of the IEEE/CVF Conference on Computer Vision and Pattern Recognition*.
- Hjort, N. L. and G. Claeskens (2003). Frequentist model average estimators. *Journal of the American Statistical Association* 98(464), 879–899.

- John Lu, Z. Q. (2010). The elements of statistical learning: Data mining, inference, and prediction. *Journal of the Royal Statistical Society Series A: Statistics in Society* 173(3), 693–694.
- Kingma, D. P. and M. Welling (2013). Auto-encoding variational bayes. arxiv [preprint]. <https://arxiv.org/abs/1312.6114> (accessed 10 December 2022).
- Krizhevsky, A. (2009). Learning multiple layers of features from tiny images. Technical report, University of Toronto.
- Krizhevsky, A., I. Sutskever, and G. E. Hinton (2017). Imagenet classification with deep convolutional neural networks. *Communications of the ACM* 60(6), 84–90.
- Le, Q. and T. Mikolov (2014). “Distributed representations of sentences and documents”. In E. P. Xing and T. Jebara (Eds.), *Proceedings of the 31st International Conference on Machine Learning*, pp. 1188–1196. PMLR.
- LeCun, Y., L. Bottou, Y. Bengio, and P. Haffner (1998). Gradient-based learning applied to document recognition. *Proceedings of the IEEE* 86(11), 2278–2324.
- Li, Q. and L. Li (2022). Integrative factor regression and its inference for multimodal data analysis. *Journal of the American Statistical Association* 117(540), 2207–2221.
- Mao, A., M. Mohri, and Y. Zhong (2023). “Cross-entropy loss functions: Theoretical analysis and applications”. In *Proceedings of the 40th International Conference on Machine Learning*.
- Mika, S., B. Schölkopf, A. Smola, K.-R. Müller, M. Scholz, and G. Rätsch (1998). Kernel pca and de-noising in feature spaces. In *Advances in Neural Information Processing Systems*, Volume 11, pp. 536–542.
- Mikolov, T., K. Chen, G. Corrado, and J. Dean (2013). Efficient estimation of word representations in vector space. arxiv [preprint]. <https://arxiv.org/abs/1301.3781> (accessed 7 September 2013).
- Ngiam, J., A. Khosla, M. Kim, J. Nam, H. Lee, and A. Y. Ng (2011). Multimodal deep learning. In *Proceedings of the 28th International Conference on International Conference on Machine Learning, ICML’11, Madison, WI, USA*, pp. 689–696. Omnipress.
- Nguyen, C. V., T. Hassner, M. Seeger, and C. Archambeau (2020). LEEP: A new measure to evaluate transferability of learned representations. In *Proceedings of the 37th International Conference on Machine Learning*, pp. 7294–7305. JMLR.
- Ouyang, L., J. Wu, X. Jiang, D. Almeida, C. Wainwright, P. Mishkin, C. Zhang, S. Agarwal, K. Slama, A. Ray, et al. (2022). Training language models to follow instructions with human feedback. *Advances in Neural Information Processing Systems* 35, 27730–27744.

- Pang, B. and L. Lee (2004). “A Sentimental education: Sentiment analysis using subjectivity summarization based on minimum cuts”. In *Proceedings of the 42nd Annual Meeting on Association for Computational Linguistics*, pp. 271–278.
- Pennington, J., R. Socher, and C. D. Manning (2014). “GloVe: Global vectors for word representation”. In A. Moschitti, B. Pang, and W. Daelemans (Eds.), *Proceedings of the 2014 Conference on Empirical Methods in Natural Language Processing*, pp. 1532–1543. Association for Computational Linguistics.
- Radford, A., J. W. Kim, T. Xu, G. Brockman, C. McLeavey, and I. Sutskever (2023). “Robust speech recognition via large-scale weak supervision”. In *Proceedings of the 40th International Conference on Machine Learning*. JMLR.org.
- Radford, A., J. Wu, R. Child, D. Luan, D. Amodei, I. Sutskever, et al. (2019). Language models are unsupervised multitask learners. *OpenAI Blog* 1(8), 9.
- Shekhar, S., V. M. Patel, N. M. Nasrabadi, and R. Chellappa (2014). Joint sparse representation for robust multimodal biometrics recognition. *IEEE Transactions on Pattern Analysis and Machine Intelligence* 36(1), 113–126.
- Shen, X., G. C. Tseng, X. Zhang, and W. H. Wong (2003). On ψ -learning. *Journal of the American Statistical Association* 98(463), 724–734.
- Vaswani, A., N. Shazeer, N. Parmar, J. Uszkoreit, L. Jones, A. N. Gomez, L. Kaiser, and I. Polosukhin (2017). Attention is all you need. In *Advances in Neural Information Processing Systems*, Volume 30, pp. 5998–6008.
- Wang, K., F. Cuzzolin, K. Shariatmadar, D. Moens, and H. Hallel (2025). Credal wrapper of model averaging for uncertainty estimation in classification. In *The Thirteenth International Conference on Learning Representations*.
- Wybo, W. A. M., M. C. Tsai, V. A. K. Tran, B. Illing, J. Jordan, A. Morrison, and W. Senn (2023). Nmda-driven dendritic modulation enables multitask representation learning in hierarchical sensory processing pathways. *Proceedings of the National Academy of Sciences* 120(32), e2300558120.
- Xie, J., R. Gao, E. Nijkamp, S.-C. Zhu, and Y. N. Wu (2020). Representation learning: A statistical perspective. *Annual Review of Statistics and Its Application* 7(1), 303–335.
- You, K., Y. Liu, J. Wang, and M. Long (2021). LogME: Practical assessment of pre-trained models for transfer learning. In *Proceedings of the 38th International Conference on Machine Learning*, Volume 139, pp. 12133–12143. PMLR.
- Yu, D., X. Zhang, and H. Liang (2024). Unified optimal model averaging with a general loss function based on cross-validation.

- Zeng, Z. and G. V. den Broeck (2023). Collapsed inference for bayesian deep learning. In *Thirty-seventh Conference on Neural Information Processing Systems*, Volume 36, pp. 78394–78411.
- Zhang, C., Z. Yang, X. He, and L. Deng (2020). Multimodal intelligence: Representation learning, information fusion, and applications. *IEEE Journal of Selected Topics in Signal Processing* 14(3), 478–493.
- Zhu, J. and T. Hastie (2005). Kernel logistic regression and the import vector machine. *Journal of Computational and Graphical Statistics* 14(1), 185–205.
- Zhu, Y., X. Shen, and C. Ye (2016). Personalized prediction and sparsity pursuit in latent factor models. *Journal of the American Statistical Association* 111(513), 241–252.